Numerical Prediction of Acoustic Sounds Occurring by the Flow Around a Circular Cylinder

Ho-Keun Kang*, Ki-Deok Ro
School of Mechanical and Aerospace Engineering, Institute of Marine Industry, Gyeongsang National University, 445 Inpyeong-dong, Tongyeong, Gyeongnam 650-160, Korea
Michihisa Tsutahara
Graduate School of Science and Technology, Kobe University, 1-1 Rokkodai, Nada, Kobe 657-8051, Japan
Young-Ho Lee
Division of Mechanical & Information Engineering, Korea Maritime University, 1 Dongsam-dong, Youngdo-ku, Pusan 606-791, Korea

Acoustic sounds generated by uniform flow around a two-dimensional circular cylinder at Re=150 are simulated by applying the finite difference lattice Boltzmann method. A third-order-accurate up-wind scheme is used for the spartial derivatives. A second-order-accurate Runge-Kutta scheme is also used for time marching. Very small acoustic pressure fluctuation, with same frequency as that of Karman vortex street, is compared with pressure fluctuation around a circular cylinder. The propagation velocity of acoustic sound shows that acoustic approaching the upstream, due to the Doppler effect in uniform flow, slowly propagates. For the downstream, on the other hand, it quickly propagates. It is also apparent that the size of sound pressure is proportional to the central distance $r^{-1/2}$ of the circular cylinder.

Key Words : Computational Fluid Dynamics, Lattice Boltzmann Method, Compressible Fluid, Acoustic Sound

Nomenclature

a : Sound velocity
c : Particle velocity
e : Internal energy
$f_i(x, t)$: Particle distribution function of fluid at lattice node x and time step t
t : Time
u_a : Fluid velocity

Greek symbols

γ : Coefficient of specific heats
μ : Viscosity
τ : Time increment
ρ : Density
ϕ : Relaxation parameter
Ω : Collision operator

* Corresponding Author,
E-mail : kang88@gaechuk.gsnu.ac.kr
TEL : +82-55-640-3064; **FAX** : +82-55-64-3128
School of Mechanical and Aerospace Engineering, Institute of Marine Industry, Gyeongsang National University, 445 Inpyeong-dong, Tongyeong, Gyeongnam 650-160, Korea. (Manuscript **Received** January 15, 2003; **Revised** April 9, 2003)

1. Introduction

With increased speed of transport vehicles like airplane, automobiles, and trains in recent years, noise has become a large environmental problem. There are two kinds of noise; vibration noise caused by the object, and fluid noise produced from the unsteady motion of fluid. The energy of sound due to object vibration is proportional to $O(10^{-2})$ of the representative velocity while the fluid noise is proportional to $O(10^{-5}\sim 10^{-8})$. Therefore, it is difficult to understand fluid noise by analyzing its mechanism.

In the numerical research of fluid sound, it can

be possible to analyze the information of the detailed flow field, which is not obtained in the experiment, by directly solving the compressible Navier-Stokes equation. However, in studying the fluid sound by a numerical method, a number of things are necessary ; a high accuracy scheme to realize the sound pressure ($O(10^{-4})$) against the static pressure, a wide calculation area to obtain far away sound pressure field, and removal of numerical reflection at the boundary.

The flow around a cylinder has been studied both experimentally and numerically for quite a while (Williamson, 1996 ; Persillon and Braze, 1998 ; Inoue, 2001) because it is one of the abundant phenomena of the fundamental fluid mechanics. Yet in spite of its simplicity, a lot of unsolved problems still exist. One of them is the generation mechanism of acoustic sound by flow around the cylinder. This has also been studied experimentally and numerically to some extent (Hardin and Lamkin, 1984). The numerical analyses have been done in the conventional way that a vorticity dominant near field is simulated first and then an acoustic far field is obtained using the approximated equations derived from the acoustic analogy (Curle, 1955).

In this paper, the far-field acoustic sounds generated from the turbulent wake of a circular cylinder at low Reynolds number is computed using the finite difference lattice Boltzmann method. The predicted sound spectra is compared with that of the other numerical simulation.

2. Theoretical Method

In the last two decades, the lattice gas method (LGM or lattice gas cellular automaton LGCA) (Frisch et al., 1987 ; Chopard and Dorz, 1998) and the lattice Boltzmann method (LBM) have become powerful tools in computational fluid dynamics (CFD). In both methods, the artificial particles move along the lattice line and collide with each other. Some books and reviews presented a lot of studies in this field (Alexander et al., 1993 ; Chen and Doolen, 1998 ; Wolf-Gladrow, 2000 ; Tsutahara and Kang, 2002).

The finite difference lattice Boltzmann method (FDLBM) developed from LBM is also one of the computational fluid mechanics methods. Cao et al. (1997) proposed this method by separating the lattice form in dispersion of space and the physical form of particle movement. It became possible and easy to simulate for the complicated object forms, and the application to various flow fields was attained. This method has high flexibility for coordinate system selection and is often the choice among various different schemes.

2.1 Thermal lattice BGK model

The lattice Bhatnager-Gross-Krook equation (BGK, 1954), a simplified version of the collision term in the lattice Boltzmann Eq. (1), is written as

$$f_i(x+c_i\tau,\ t+\tau)=f_i(x,\ t)+\Omega_i \tag{1}$$

Here, the real number $f_i(x,\ t)$ is the mass of fluid at each lattice node x and time step t, moving in direction i.

The discrete lattice BGK equation, a simplified version of the discrete lattice Boltzmann equation, is used.

$$\frac{\partial f_i(x,\ t)}{\partial t}+c_{i\alpha}\frac{\partial f_i(x,\ t)}{\partial x_\alpha}=\Omega_i \tag{2}$$

The microscopic dynamics associated with Eq. (2) can be viewed as a two-step process of movement and collision. In the collision step, the distribution functions at each site relax toward a state of local equilibrium. For simplicity, the linear, single time relaxation model of BGK that has been widely applied to LBM is used as follows.

$$\Omega_i=-\frac{1}{\phi}\left[f_i(x,\ t)-f_i^{(0)}(x,\ t)\right] \tag{3}$$

The collision operator Ω_i conserves local mass, momentum, and kinetic energy while the relaxation parameter ϕ controls the rate at which the system relaxes to the local equilibrium of $f_i^{(0)}(x,\ t)$.

The local equilibrium distribution function in Eq. (2) is expressed as according to Kang et al. (2002).

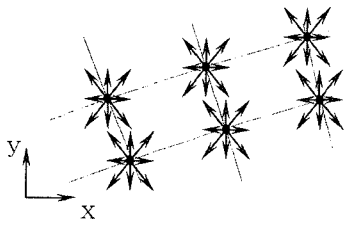

Fig. 1 Two-dimensional space and particle distribution in FDLBM

$$f_i^{(0)}=F_i\rho\left[1-2Bc_{i\alpha}u_\alpha+2B^2(c_{i\alpha}u_\alpha)+Bu^2-\frac{4}{3}B^3(c_{i\alpha}u_\alpha)^3-2B^2c_{i\alpha}u_\alpha u^2\right] \quad (4)$$

The moving particles are allowed to move with five kinds of speed c, $2c$, $3c$, $\sqrt{2}c$ and $2\sqrt{3}c$. Figure 1 shows a two-dimensional space lattice.

2.2 Finite difference lattice boltzmann method

The models for compressible fluids are sometimes unstable in calculation because the distribution function gives a negative value. Using the finite difference considerably stabilizes the calculation (Cao et al., 1997; Seta et al., 1998).

For this purpose, this paper employs the discretized BGK Eq. (2). This equation is shown to lead the Navier-Stokes equations by the Chapman-Enskog expansion, and the term $(\phi-1/2)$ in transfer coefficient changes into ϕ. The relationship between the kinematic viscosity and the relaxation time factor becomes

$$\mu=\frac{2}{D}\rho e\phi \quad (5)$$

For high Reynolds number flows which are very important in engineering fields, $\mu\ll1$ must be satisfied. If Euler's first order forward difference scheme is used for time integral, the equation is transformed as;

$$f_i(x+c_i\tau,\ t+\tau)=f_i(x,\ t)+\Delta t\left[-c_{i\alpha}\frac{\partial f_i(x,\ t)}{\partial x_\alpha}-\frac{1}{\phi}f_i^{(0)}(x,\ t)\right] \quad (6)$$

where Δt is the time increment. From the condition of stability in Eq. (6), the following condition must be satisfied.

$$\frac{\Delta t}{\phi}<2.0 \quad (7)$$

This states that the distribution function approaches its equilibrium state by every collision. Relations Eq. (5) and (7) lead that for high Reynolds number flows, the time increment chosen must be very small and the calculation time will be very long.

Therefore, an equation in which the third term is added to the discretized BGK equation (Eq. (2)) is introduced (Kang et al., 2002);

$$\frac{\partial f_i(x,\ t)}{\partial t}+c_{i\alpha}\frac{\partial f_i(x,\ t)}{\partial x_\alpha}-\frac{Ac_{i\alpha}}{\phi}\frac{\partial}{\partial x_\alpha}[f_i(x,\ t)-f_i^{(0)}(x,\ t)]=-\frac{1}{\phi}[f_i(x,\ t)-f_i^{(0)}(x,\ t)] \quad (8)$$

where $A(>0)$ is a constant. Then the relationship changes to

$$\mu=\frac{2}{D}\rho e(\phi-A) \quad (9)$$

and if an appropriate value of A is chosen, there will be a large enough ϕ for flows of small viscosity, time increment can also be made large enough.

3. Numerical Procedure

A schematic diagram of the flow around a two-dimensional circular cylinder is presented in Fig. 2. In the Cartesian coordinate $(x,\ y)$, the uniform flow of the velocity U_0 parallel to the x direction is considered. Normalized by the static sound velocity a_0, the streamwise velocity is prescribed by the Mach number M.

$$M=\frac{U_0}{a_0}=\frac{U_0}{\sqrt{2e}} \quad (10)$$

Furthermore, the cylinder of the diameter d is fixed at the origin. The polar coordinates $(r,\ \theta)$ are also used, where the azimuthal angle θ is defined from upstream in the clockwise direction. The Reynolds number is defined as $\mathrm{Re}=U_0d/\mu$ where μ is the kinematic viscosity. Flow quantities are non-dimensionalized by d, a_0, and ρ_0, where ρ_0 is the ambient density. The physical parameter prescribed is the ratio of specific heats $\gamma=(D+2)/D$.

A third-order-accurate up-wind scheme (second-order-accurate at the boundary) is used for

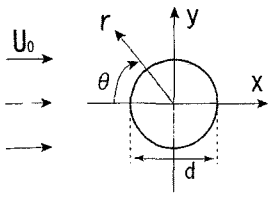

Fig. 2 Schematic diagram of the flow model

spatial derivatives, and a second-order-accurate Runge-Kutta scheme is used for time integration. Adiabatic and no-slip conditions are adopted on the cylinder surface. Non-reflecting boundary conditions (Pointsot and Lele, 1992) are adopted on the outer boundary so that the numerical wave reflections from the boundary are removed. Initial flows are given as potential flows except for the boundary layer on the cylinder wall.

The non-uniform O-grid systems are applied to simulate the entire field from near to far acoustic fields. A typical grid system in the case of Re= 150 is constructed as follows: the number of the grid points results in $r \times \theta = 201$ (in the radial direction) $\times 121$ (in the azimuthal direction); the time Δt is 0.02; and the examined Mach numbers use the sound velocity by changing the internal energy e. All the calculations are in two-dimension and use 2D21V model.

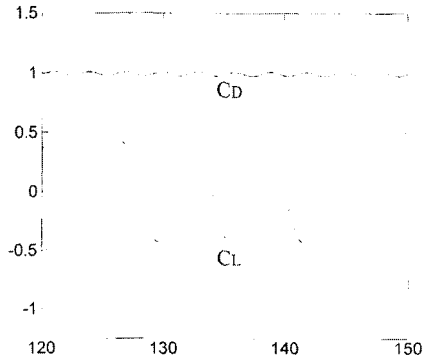

Fig. 3 Time history of drag C_D and lift coefficient C_L. Re=150, M=0.2

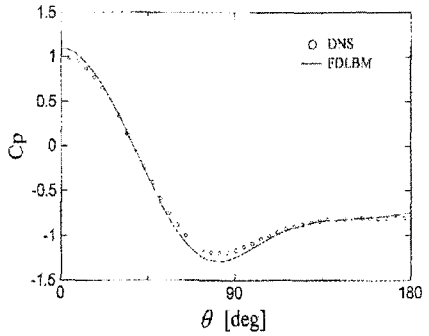

Fig. 4 Comparison of pressure coefficient C_p between FDLBM and DNS at $0 \leq \theta \leq \pi$. Re= 150, M=0.2

4. Results and Discussion

Direct simulation of acoustic waves emitted from a circular cylinder in a uniform flow is performed using the proposed model (Eq. (8)), in which the cylindrical coordinated system is employed.

The numerical results when the Karman vortex street is fully developed are shown in Figs. 3 to 8 in case of Re=150 and M=0.2.

Figure 3 depicts the forces on the cylinder surface, which are regarded as main sound sources by theory (Curle, 1955). Time histories of drag coefficient C_D and lift coefficient C_L are also represented in Fig. 3. They are defined as the ratio of the forces to the kinematic energy at infinity, $\rho_0 U^2/2 = M^2/2$. The mean value of the drag coefficient, $\overline{C_D}$, is about 1.01. Figure 4 presents the mean and fluctuating surface pressure as a function of the azimuthal angle θ with that of DNS (Inoue, 1999). Pressure coefficient C_p is the time averaged pressure on the cylinder surface normalized by the value at the stagnation point $\theta = 0^0$. A comparison of the pressure coefficient at $0 \leq \theta \leq \pi$ indicates that FDLBM is compatible with DNS.

The acoustic sounds in the far field are compared with the forces on the cylinder. Here, the sound pressure Δp is defined as

$$\Delta p = \frac{p - p_0}{p_0} = \frac{p - \rho_0 e_0}{\rho_0 e_0} \tag{11}$$

where p_0 denotes the ambient pressure. Time history Δt of sound pressure at the point d=50 and θ=90° and −90° is shown in Fig. 5. By comparing with the lift coefficient C_L in Fig. 3, it can be seen that Δp oscillates at the same frequency as the vortex shedding frequency.

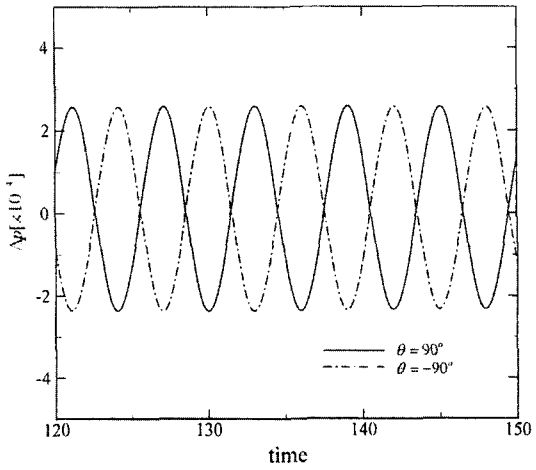

Fig. 5 Time history of sound pressure at $d=50.3$, and $-90°$

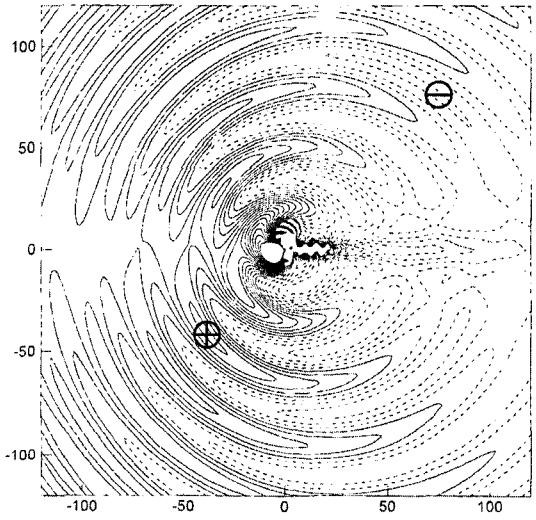

Fig. 6 Contours of sound pressure by FDLBM at t= 133. Re=150, $M=0.2$. The pressure contour level is $-3.0\times10^{-4}\leq\Delta p\leq3.0\times10^{-4}$. Solid lines : positive, dotted : negative

The Strouhal number is defined by $S_t=fd/U$ where f is the frequency of the periodic vortex shedding. It is evaluated at $S_t=0.178$, which is very close to the experimental result for Re=150 (Williamson, 1996).

Figure 6 shows the acoustic pressure field at $t=133$, where the contour level fluctuates $\Delta p_{step}=3\times10^{-4}$. The solid lines indicate the positive pressures and the dashed lines are the negative ones. As can be seen from this figure, rarefaction

Table 1 Numerical results of speed of sound at each direction ($M=2.0$)

θ	cos θ	$\tilde{a}_\theta=a_\theta/U_0$	Δr	$\Delta r/\tilde{a}_\theta$
45.0	0.707	4.293	4.277	0.996
90.0	0.0	5.00	4.891	0.978
135.0	−0.707	5.707	5.585	0.979

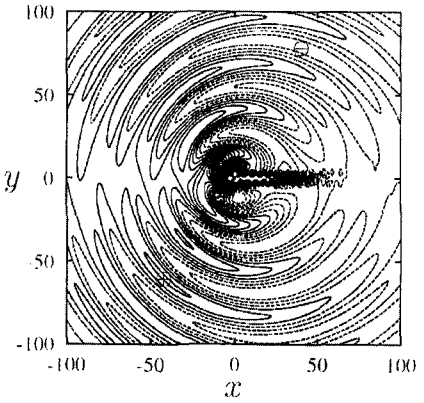

Fig. 7 Contours of sound pressure by DNS. Re= 150, $M=0.2$. The calculation domain was given at $r\times\theta=871\times503$ (Inoue, 2001)

waves with negative Δp and compression waves with positive Δp are generated alternately around the cylinder at the origin, and propagate downstream and upstream, respectively. Behind the cylinder, vortices become weaker with increasing downstream distance, and the influence of the far wake on the sound field appears only in the sound propagating toward downstream around $\theta=0^0\sim180°$. This result is consistent with the acoustic pressure field by DNS (Inoue, 2001), which is shown in Fig. 7, and compatible with that of FDLBM.

Table 1 shows the difference between the theoretical prediction and the calculated value of the propagation speeds. At all directions, the propagation speeds vary $a_\theta=a_s-U_0\cos\theta$ by mean flow of the medium. In this case, the estimated error is within 2.1% and the results agree well with the theoretical predictions.

Figure 8 illustrates the distributions and decays of the sound pressure plotted along the various directions ($\theta=45°$, 90° and 135°). The distribution of Δp are plotted against the radial distance

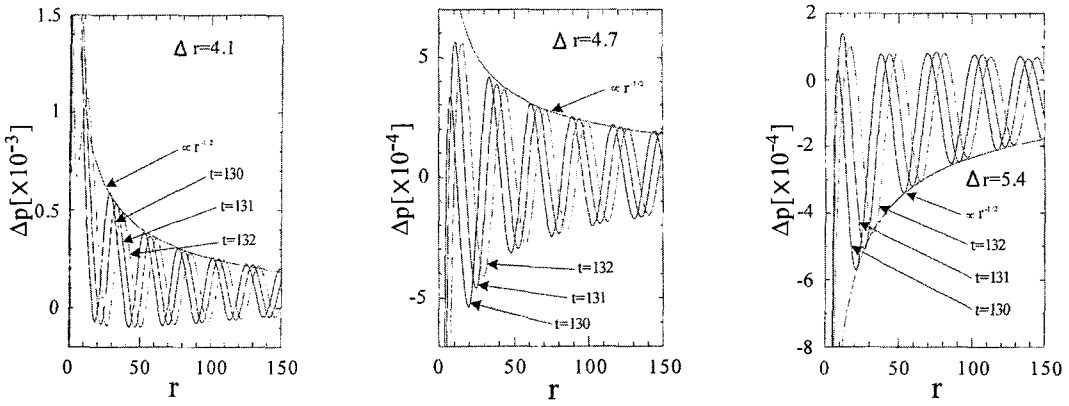

Fig. 8 Distributions and decays of sound pressure. Re=150, M=0.2

r from the origin at the three different times t=130, 131, and 132. Each peak of the waves is found to propagate and decay. The propagation speed of the waves is equal to the speed of sound in the far field, in agreement with the linear acoustic theory. Also, the decaying curves are converged to the lines proportional to $r^{-1/2}$ in the far field, which is again in accordance with the theory. These results suggest that the sounds generated from the cylinder at low Reynolds numbers are precisely captured by FDLBM if both the flow dynamics in the near field and the wave propagations in the far field are computed with high accuracy.

5. Concluding Remarks

The acoustic sounds generated from the flow around the circular cylinder are successfully simulated using the FDLBM of the two-dimensional 21velocity model. The sound frequency is the same as the vortex shedding frequency of the Karman vortex street. The rarefaction waves and the compression waves are alternately generated and propagate toward downstream and upstream, respectively. The sound pressure also decays proportional to $r^{-1/2}$ in the far acoustic field, which agrees with the theoretical prediction.

Acknowledgment

This work was supported by the Brain Korea 21 Project.

References

Alexander, F. J., Chen, S. and Sterling, D. J., 1993, "Lattice Boltzmann Thermodynamics," *Physical Review* E, Vol. 47, pp. 2249~2252.

Bhatnagar, P. L., Gross, E. P. and Krook, M., 1954, "A Model for Collision Processes in Gases. I. Small Amplitude Processes in Charged and Neutral One-Component Systems," *Physical Review*, Vol. 94, pp. 511~525.

Cao, N., Chen, S., Jin, S. and Martinez, D., 1997, "Physical Symmetry and Lattice Symmetry in the Lattice Boltzmann Method," *Physical Review* E, 55, pp. R21~R24.

Chen, Y. and Doolen, G. D., 1998, "Lattice Boltzmann Method for Fluid Flows," *Annual Review Fluid Mechanics*, Vol. 30, pp. 329~364.

Chopard, B. and Droz, M., 1998, *Cellular Automata Modeling of Physical Systems*, Cambridge University Press.

Curle, N., 1955, "The Influence of Solid Boundaries upon Aerodynamic Sound," *Proceeding Royal Society* A231, pp. 505~514.

Frisch, U., Hasslacher, B. and Pomeau, Y., 1986, "Lattice-Gas Automata for the Navier-Stokes Equation," *Physical Review Letters*, Vol. 55, pp. 1505~1508.

Hardin, J. C. and Lamkin, S. L., 1984, "Aeroacoustic Computation of Cylinder Wake Flow," *AIAA Journal*, Vol. 22, pp. 51~57.

Inoue, O., 2001, "Direct Numerical Simulation of Sound," *Japan Society of Fluid Mechanics*, Vol. 20, pp. 187~195.

Kang, H. K., Tsutahara, M., Ro, K. D. and Lee, Y. H., 2002, "Numerical Simulation of Shock Wave Propagation using the Finite Difference Lattice Boltzmann Method," *KSME International Journal*, Vol 16, No 10, pp. 1327~1335.

Persillon, H. and Braza, M., 1998, "Physical Analysis of the Transition to Turbulence in the Wake of a Circular Cylinder by Three-dimensional Navier-Stokes Simulation," *Journal of Fluid Mechanics*, Vol. 365, pp. 23~88.

Pointsot, T. and Lele, S. K., 1992, "Boundary Conditions for Direct Simulation of Compressible Viscous Flows," *Journal of Computational Physics*, 101, pp. 104~129.

Seta, T., Kono, K., Martinez, D. and Chen, S., 1999, "Lattice Botlzmann Scheme for Simulating Two-Phase Flows," *Trans. JSME Journal*, B, 65-634, pp. 1955~1963.

Tsutahara, M. and Kang, H. K., 2002, "A Discrete Effect of the Thermal Lattice BGK Model," *Journal of Statistical Physics*, Vol. 107, No. 112, pp. 479~498.

Williamson, C. H. K., 1996, "Vortex Dynamics in the Cylinder Wake," *Annual Review of Fluid Mechanics*, Vol. 28, pp. 477~539.

Wolf-Gladrow, D. A., 2000, *Lattice-Gas Cellular Automata and Lattice Boltmann Models*, Lecture Notes in Mathematics, Springer.